71st International Astronautical Congress (IAC) – The CyberSpace Edition, 12-14 October 2020.

IAC-20,E2,3-GTS.4,10,x60846

Critical design of a MoonFibre experimental apparatus for the use on a REXUS sounding rocket

Stefan Panajotović* [a], **Leon Wiesen** [a], **Lukas Rodeck** [a], **Gerrit Niehuss** [b], **Jonathan Schott-Vaupel** [b], **Johannes Hoormann** [a], **Robin Duhnsen** [a], **Robert Sternschulte** [a], **Jaspar Meister** [a], **Maximilian Schirp-Schoenen** [a], **Caroline Krämer** [a], **Ines Gehring** [a], **Anthony Pham** [a], **Felix Gertdenken**, **Sunny Singh** [a], **Jannis Bergmann** [a], **Can Özmaden** [a], **Leon Dülberg** [a]

[a] *RWTH Aachen University, Germany*
[b] *FH Aachen University of Applied Sciences*
* Corresponding Author, stefan.panajotovic@rwth-aachen.de

Abstract

Space industry experiences new interest to return to the Moon in this decade. Different entities aim to mine lunar resources, perform scientific experiments and build orbital and surface stations. Building lunar bases using only Earth-sourced materials is too expensive. The common approach to solve this problem is the In-Situ Resource Utilization. By utilizing local resources, various products can be created and put in service directly on the Moon. One type of such materials is fiber-based, developed within the *MoonFibre* project of RWTH Aachen University. Current *MoonFibre* are produced using a conventional spinning apparatus and lunar simulant. While these are similar in composition to terrestrial basalt fibers, *MoonFibre* will be produced entirely of lunar regolith on the Moon surface, requiring only energy as additional input. *MoonFibre*-based products can then be utilized as structural reinforcement, hydroponic substrates or thermal insulation, thus contributing to a sustainable and affordable lunar settlement.

The terrestrial basalt-fiber spinning process is well developed. To this author's knowledge however, spinning continuous basalt fibers in space environment has never been attempted before. This paper presents a final design of an experimental spinning apparatus. This apparatus is to be launched on a REXUS sounding rocket providing three minutes of experiment time in microgravity conditions. Spinning of *MoonFibre* will be attempted in space environment for the first time.

The experiment fits inside a 356 mm diameter module with a height of 220 mm. Terrestrial spinning facilities are much larger and require extensive manpower for operation. Gravity forces the molten basalt from the oven through multiple nozzles, at which point the melt is quenched and fibers are created. Instead, this experimental design uses centrifugal forces to push the melt through two nozzles placed opposite of each other by rotating the oven. The spinning apparatus is placed inside a pressure vessel. As it leaves the nozzles, molten simulant is quenched by air pressurized at 1 bar. To prevent components from overheating, air circulates between the pressure vessel and a heat sink, where heat is stored latently using a phase change material. A camera is used to confirm successful creation of fibers already during the flight. The fibers are collected inside the experiment module and will be recovered for post-flight analysis.

This experiment, designed entirely by a team of students, serves as a proof of concept and will provide vital insight of how gravity influences the spinning process and the mechanical properties of *MoonFibre*.

Keywords: ISRU, Moon, lunar exploration, *MoonFibre*, REXUS, microgravity

Acronyms/Abbreviations

ISRU - in-situ resource utilization
ITA - Institut für Textiltechnik of RWTH Aachen University
SLA - Structural Mechanics and Lightweight Design of RWTH Aachen University
ITALUS - ITA Lunar Simulant
EVA - Extra Vehicular Activity
IMFEX - ISRU MoonFibre Experiment
REXUS - Rocket Experiments for University Students
PCM - phase change material
CCU - central control unit
PtRh – Platinum-Rhodium

1. Introduction

The main objective on NASA's currently planned Artemis program is to perform human landing on the Moon by 2024 and establish a sustainable lunar base by 2028. [1] In order to reach this long-term goal, costs for building and maintaining such a station must be reduced to a minimum. These costs will be kept minimal by employing commercial landers [2]. Nonetheless, costs per kilogram delivered to the lunar surface will likely remain high, by some estimates even 890.000 $/kg [3]. Widely accepted approach to reduce these costs is by employ in-situ resource utilization (ISRU) technologies [4]. By using lunar resources to produce various products directly on the Moon, expensive launches from Earth can be avoided to some extent.

Such an ISRU technology developed at the RWTH Aachen University by the Institut für Textiltechnik (ITA) and the Institute for Structural Mechanics and Lightweight Design (SLA) is the MoonFibre technology [5]. The aim of the MoonFibre project is to produce fiber-based resources from Moon regolith directly on the lunar surface. Using these fibers, a range of products can be manufactured that would otherwise have to be brought from Earth. These products can then be utilized with the larger context of a permanent lunar base. The same technology can be utilized similarly on Mars. Possible use-cases for MoonFibre products include hydroponic substrates, filters, reinforcement of structural habitat components, production of mechanical elements such as gears and axles and settlement equipment such as astronaut clothing and protective coveralls for EVA (Extra Vehicular Activity) suits. [5]

Due to the scarcity of the lunar regolith that has been brought from Earth during previous missions, no fibers from real regolith have been spun yet. Previous work done on ITA [9] investigated the fiber spinning process with two in-house made regolith simulants called ITALUS-1 and ITALUS-2 (ITA Lunar Simulant) [6]. It was shown that the production of fibers from these simulants is possible and that the mechanical properties of such fibers are comparable to terrestrial basalt fibers. Fig. 1 and Fig. 2 show the microscopic and macroscopic images of fibers produced using the ITALUS-2 simulant.

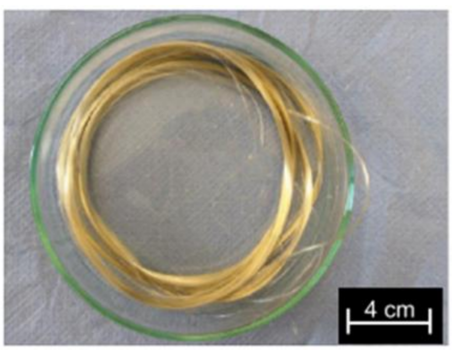

Fig. 1: Macroscopic view of fibers made from ITALUS-2 [6]

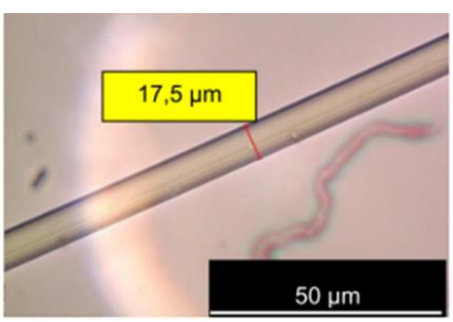

Fig. 2: Microscopic view of fibers made from ITALUS-2 [6]

The spinning process of basalt fibers on Earth is shown in Fig. 3. Feedstock material is fed into a melting oven called bushing. There it is molten at more than 1200 °C. The bushing is made of an inert Platin-Rhodium alloy. Once the feedstock material is molten, it leaves the bushing through multiple nozzles on the bushing's lower side. The molten material is pulled by the force of gravity and by the rotating winder placed below the bushing. Molten material is quenched once it leaves the bushing using cooling fins and a water spray cooling system to avoid crystallization and create an amorphous structure. To avoid damage to the fibers due to friction and to improve chemical bonding between them, they are passed by equipment for static discharging and sizing. The produced continuous fibers can have a diameter as small as 15 µm. [5]

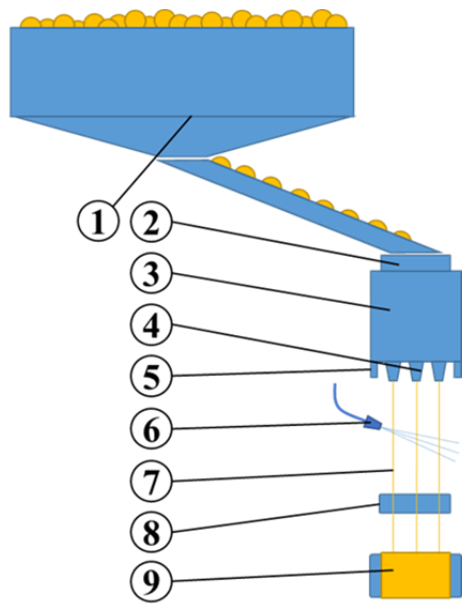

Fig. 3: Terrestrial basalt fiber spinning process; (1) – Raw material supply, (2) – Feeding & dosing system, (3) – Bushing , (4) – Nozzles, (5) – Cooling fins, (6) – Water spray for static discharging, (7) – Fibers, (8) – Sizing applicator, (9) – Rotating winder. [5]

This spinning process is adapted for usage in Earth. Gravitational force is needed to feed raw material and push the fibers from the nozzle. Convection through the atmosphere is needed to cool the fibers once they leave the nozzle and a water jet is used for static discharging. Therefore, the terrestrial spinning process cannot be utilized in vacuum and low or microgravity. The whole process has a low level of autonomy and requires constant active monitoring and control. Lastly, these spinning machines are multiple stories high and they weigh multiple tons. [5] The main challenges of the MoonFibre project are to adapt this spinning process for the lunar environment and to develop a miniaturized and autonomous spinning facility which can be utilized on the Moon. [7] Fig. 4 shows such a spinning facility. [5]

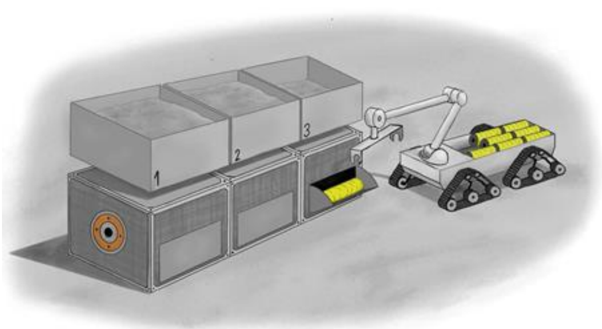

Fig. 4: MoonFibre spinning facility on the Moon [5]

Apart from ZBLAN [8], no fiber material has ever been spun in space environment, where ZBLAN are optical fibers and have different production process than structural fibers such as MoonFibre. As the first step in designing a MoonFibre spinning facility capable of operating in space, the ISRU *MoonFibre* Experiment (IMFEX) project was initiated. The mission objective of IMFEX is to design a spinning facility and launch it on a suborbital flight into space on-board a REXUS 30 (Rocket Experiments for University Students) sounding rocket.

The REXUS program is a German-Swedish program enabling students from European universities to launch scientific and technological microgravity experiments on suborbital flights. REXUS rockets are single-stage rockets powered by the Improved Orion solid rocket engine. REXUS measures 5.6 m in length and 356 mm in diameter with a maximum payload of 95 kg. Approximately 3 minutes of spaceflight and altitudes of between 78 and 93 km can be reached. Two REXUS rockets are launched each year from Esrange Space Centre in northern Sweden. The experiments are recovered after flight and can be analyzed further. Fig. 5 depicts the REXUS rocket. [9]

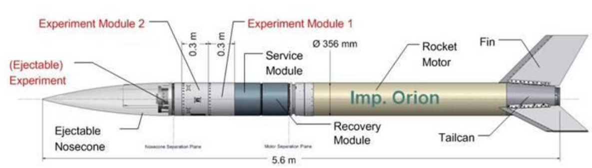

Fig. 5: A depiction of REXUS sounding rocket [9]

Within these 3 minutes, the spinning of structural fibers from lunar regolith simulant will be attempted in space environment for the first time. These fibers will be recovered post-flight, their mechanical properties analyzed and compared to fibers made by the same spinning facility on the ground. Lessons learned from IMFEX project are to be used as input for future developments of lunar spinning facilities. Exact objectives, requirements and preliminary experiment design was presented in previous work by *Krämer et al* [7]. This paper instead focuses on the IMFEX final design and presents first results from initial verification tests.

2. Final Experiment Design

This section will describe the final design of IMFEX centrifugal spinning apparatus. Spinning basalt fibers using centrifugal forces in microgravity conditions is to these author's knowledge the first of its kind. The experiment overview with all the main sub-assemblies is shown on Fig. 6.:

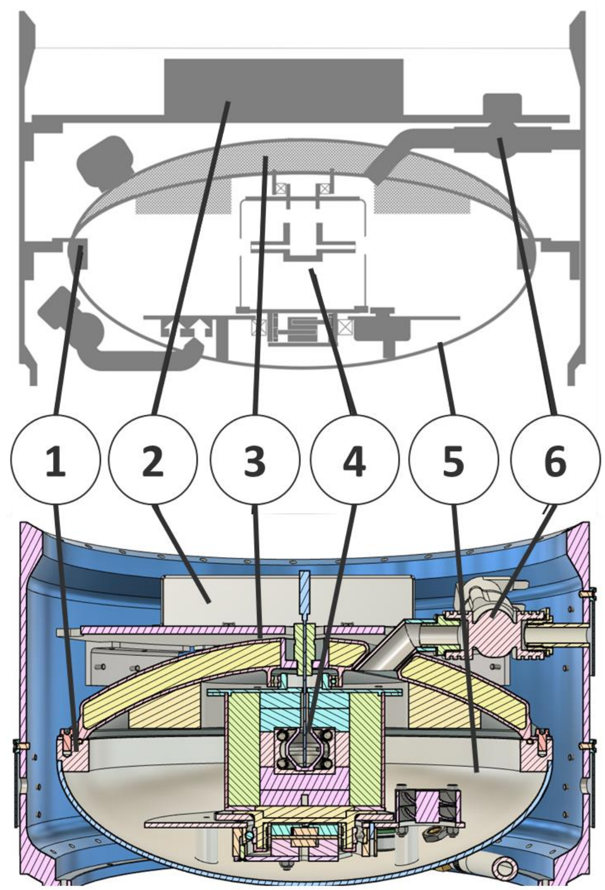

Fig. 6: IMFEX concept: Schematic view (Top) and CAD rendering (Bottom); (1) – Fixed drum, (2) – Computer compartment, (3) – Heat sink, (4) – Bushing assembly, (5) – Pressure vessel, (6) – Hot side valve

The centerpiece of the IMFEX spinning apparatus is a rotating bushing assembly. It is heated by a heating wire and thermally isolated using a combination UltraBoard® and Promalight® high-performance insulation materials. Lunar regolith simulant is placed inside the Platinum Rhodium (PtRh) bushing pre-flight. The heating system will be turned on 20 minutes before lift-off and it will melt the simulant before launch. During the flight, temperature of the simulant will be held constant and turned off only 5 minutes into the flight, when the microgravity phase of the flight is over. Upon reaching microgravity conditions, the bushing is spun up to the intended speed and the centrifugal forces will push the molten simulant through two nozzles located opposite of each other at the wall of the bushing. To generate a sufficient mass flux of molten simulant (about 105 kg/s per nozzle) the bushing shall rotate with 600 rpm. Depending on the rotational speed of the bushing, the fiber diameter can be varied. Heating power is provided using a rotational power supply using copper rings and brushes. Detailed design of the rotational bushing assembly is shown on Fig. 7. Fig. 8 shows the PtRh bushing 3D-printed by Cooksongold.

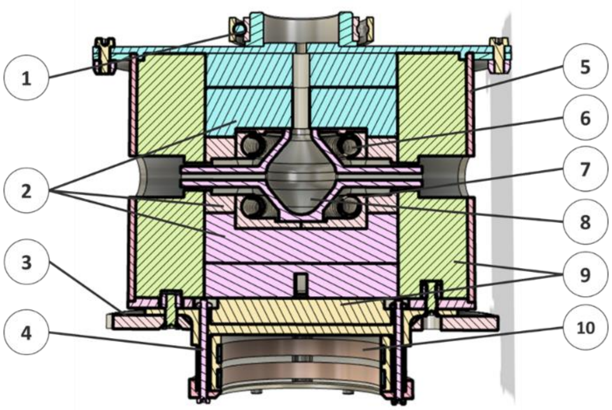

Fig. 7: Rotational bushing assembly; (1) – Bearing Mount, (2) – UltraBoard® Isolation, (3) – Drive Gear, (4) – Bottom Bearing Mount, (5) – Aluminum Housing, (6) – Heating Wire, (7) – Ceramic insulation holding the bushing and the heating wire, (8) – PtRh Bushing, (9) – Promalight® Isolation, (10) – Rotational power supply

Fig. 8: PtRh bushing 3D-printed by Cooksongold

Initial design foresaw another rotor surrounding the bushing assembly. It was supposed to spin in the opposite direction and act like a catching drum for the fibers, replacing the winder used in terrestrial spinning facilities. Initial tests showed that this was redundant and that such rotating catching drum does not improve the ability of the spinning facility to pull the fibers from the bushing. It was therefore replaced by a stationary screen of aluminum, which fibers will hit as they leave the bushing nozzles. Even if a fiber snaps, no particular action is needed to restart the process. New fibers can simply be spun over the previous ones. Advantage of this design is that it can be operated in both Earth's gravity as well as in microgravity. This will allow comparison between fibers spun in both environments. About 1.4 km of fibers are expected to be produced during 3 minutes of experiment duration. The preliminary design also foresaw a bushing closing system, which was supposed to prevent hot melt from leaving the bushing upon experiment shutdown and possibly damaging other components. Initial tests have also shown that this system is unnecessary, since no melt can leave the nozzles as soon as the heating system is turned off. The bushing and the drivetrain are placed inside a pressure vessel and are operated within an air atmosphere at room temperature and the constant pressure of 1 bar. This way forced convection quenches the fibers before they are deposed on the stationary catching drum. The cooling of the experiment saw major changes when compared to the preliminary design as depicted on the Fig. 9:

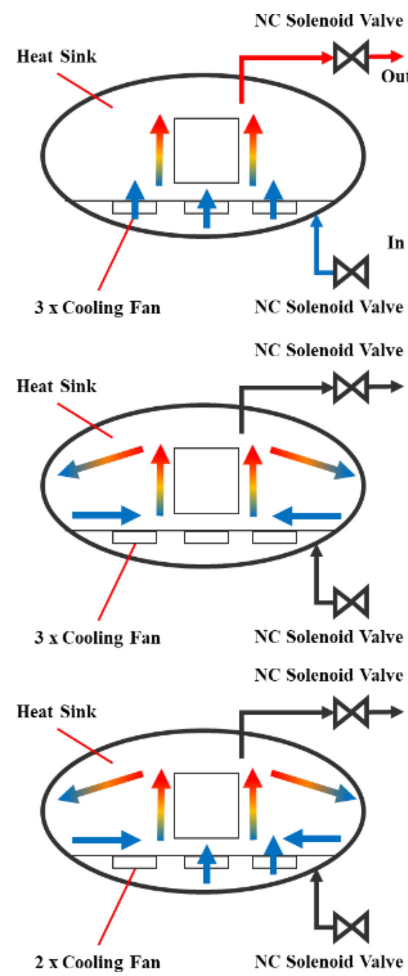

Fig. 9: Final concept of the IMFEX cooling system; Top – Pre-heating phase before launch; Middle – Cooling

phase during the powered flight; Bottom – Cooling phase during microgravity experiment time;

As it can be seen from Fig. 9, there are three experiment phases that need to be accounted for the cooling system. During the pre-heating procedure, while the rocket is still on the launch pad, cold air will be sucked using three cooling fans from the environment and circulated through the pressure vessel. It is then vented overboard using the outlet on the upper part of the pressure vessel. Shortly before launch, the solenoid valves will close of the pressure vessel. During the powered flight air will be circulated using only natural convection. Upon reaching microgravity, forced convection will be created using two out of three cooling fans. The third will be left open to allow the air to circulate. The whole pressure vessel assembly is shown on Fig. 10:

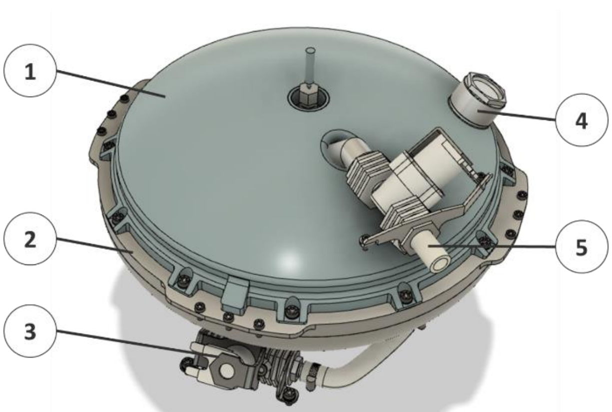

Fig. 10: Whole pressure vessel with the tubing of the cooling system; (1) – Heat Sink; (2) – Lower side of the pressure vessel; (3) – cool side tubing and valve; (4) – Heat Sink PCM Inlet; (5) – hot side tubing and valve.

Heat from the hot air will be stored latently [10] using the heat sink integrated into the top part of the pressure vessel. The heat sink contains 600 g of paraffin wax phase change material (PCM) [11]. In order to assure uniform heat transfer throughout the PCM, lattice structure was implemented inside the heat sink. This lattice structure also serves as structural reinforcement of the heat sink. The same lattice structure was added on the lower side of the heat sink in order to increase the surface used for the heat transfer from the hot air to the heat sink. Ultimately, the fiber temperature must be reduced from 1260 °C to 690 °C with a cooling rate which ensures optimal mechanical properties of the fibers. The cooling rate depends on multiple factors, such as basalt composition or heating conditions. Analytical models for the optimal cooling rate do not deliver similar results as the ones empirically obtained [12, 13]. The final heat sink design is depicted in Fig. 11:

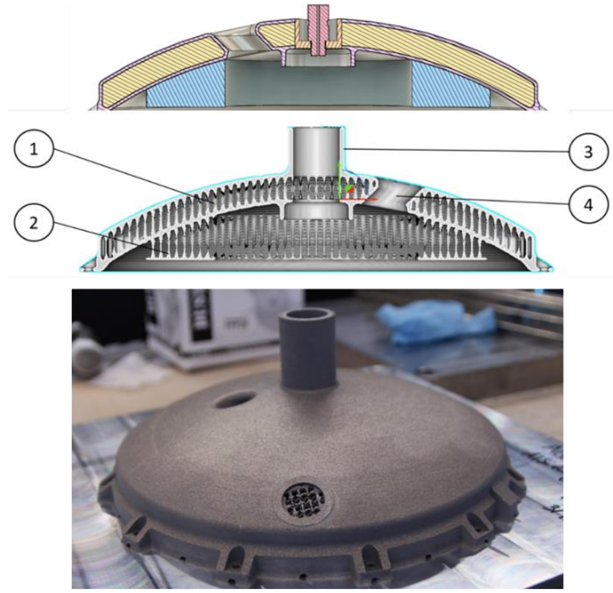

Fig. 11: CAD heat sink part in with simplified lattice structure (Top); Rendered lattice structure (Middle), (1) – Internal lattice structure, (2) – External lattice structure, (3) – Duct for manufacturing purposes, (4) – Cooling pipe passthrough; Note that the lattice structure is shown as vertical lines on the lower picture; Heat sink as printed by the EOS GmbH before the post-processing (Bottom)

An action cam mounted on the pressure vessel monitors the spinning process and saves images. Another camera observes the catching drum and detects whether fibers are collected. These information as well as sensor information can be transmitted to the ground station during flight. A sensor system gathers avionics telemetry, pressure and the temperature within the pressure vessel, temperature inside the bushing and temperature of the heat sink. The latter is measured at 8 different locations for additional information about its performance in flight. This data is forwarded to the central control unit (CCU). The control system consists of a motor control unit, a heating control unit, a computer and a data processing system. At the end of the experiment period computer vision edited images of the fiber screen are transmitted in case the experiment cannot be recovered. Schematics of the electronics system is shown in Fig. 12: [7]

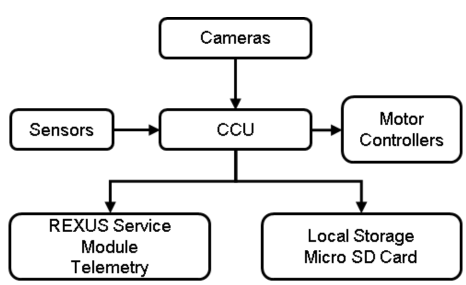

Fig. 12: Schematics of the electronics system [7]

The experiment's power system consists of an external power supply and an on-board secondary battery. The bushing will be heated up on the launch pad using the external power supply. Shortly before take-off, the system will switch to internal power using LiPO batteries instead of NiMH batteries that were initially planned.

The system including the experiment module has an overall mass of 14. 1 kg, 348 mm in diameter and 220 mm in height.

3. Concept verification

Multiple simple prototypes were built during the design process to verify functional principles of the experiment. Special attention was set on the bushing heating system, the experiment cooling system and on the centrifugal spinning apparatus. This section will describe some of the tests that were performed.

3.1. Heating system tests

First tests that were performed verified the bushing heating system using a 0.6 mm Kanthal AR heating wire. A dummy steel bushing was manufactured for this purpose. This bushing together with the heating wire were embedded in UltraBoard® material and heated up using external power supply. Multiple iterations of this test was performed, gradually increasing the heating power and heating temperature. Second iteration of this test is shown in Fig. 12 and Fig. 13:

Fig. 11: The econd prototype of a stainless-steel bushing embedded in UltraBoard® material surrounded by Kanthal AR heating wire

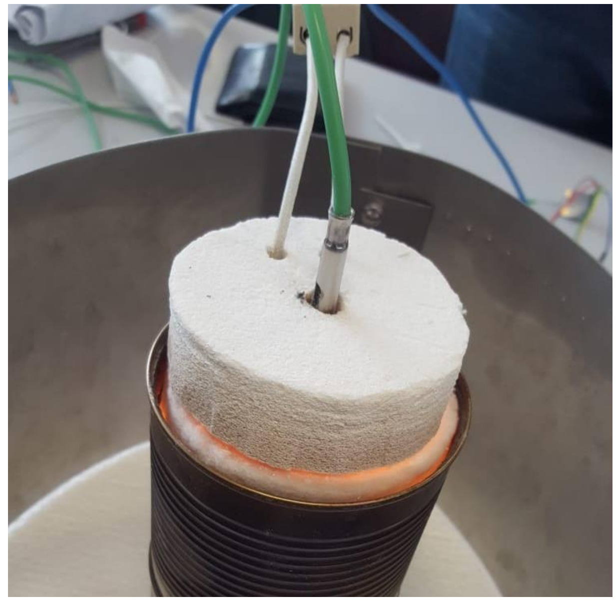

Fig. 13: The second prototype during the heating procedure, reaching 1200 °C after 1000s of constant heating with 183 W at 5 A.

While these initial tests showed that the heating system concept is valid, the heating wire proved to be brittle after being heated to 1200 °C. During the spinning tests that will be described in the next chapter, the heating wire broke after approximately 15 minutes into the tests, due to the vibrations induced by the spinning apparatus. Due to the imprecise winding of the heating wire, it is likely that coils were in contact with each other, thus causing a short circuit. Lastly, it is likely that imperfections in the wire lead to faster failure after it was exposed to thermal stresses. It was concluded that Kanthal A1 heating wire, which can reach temperatures of 1350 °C, of thicker diameter of 1 mm should be used for the flight hardware. Fig. 14 shows the Kanthal AR wire after heating under the microscope.

Fig. 14: 0.6 mm Kanthal AR wire after heating under the microscope. Note the reduction of the diameter of the wire as well as the spot where the wire oxidized and eventually failed.

3.2. Spinning apparatus tests

After the initial heating tests have shown that temperatures of 1200 °C can be reached, the team mounted the above-shown heating assembly on a simple spinning apparatus in order to attempt spinning of glass fibers. For the first spinning tests, E-glass was used instead of regolith simulant. The latter has higher melting temperature which were unable to be reached using this simple prototype. Fig. 15 shows 5 g E-glass inside the stainless-steel bushing. Fig. 16 shows the simple prototype of the spinning apparatus.

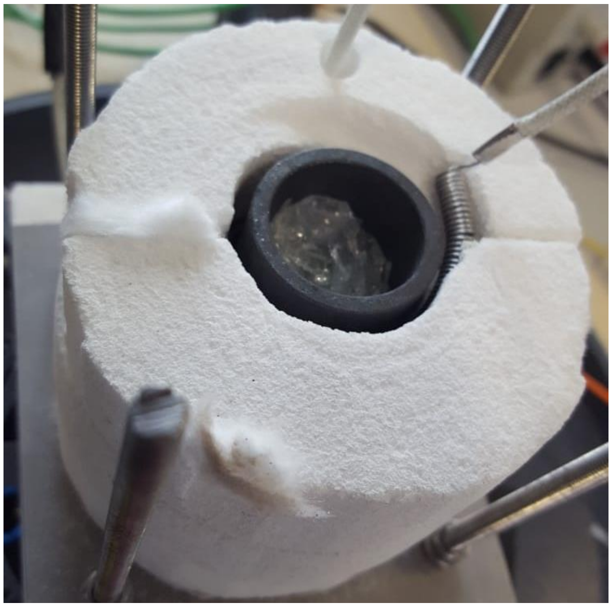

Fig. 15: Bushing assembly with the heating wire and thermal insulation for the first attempt at spinning the E-glass fibers. Temperatures reached were 1180 °C using 200 W at 5 A.

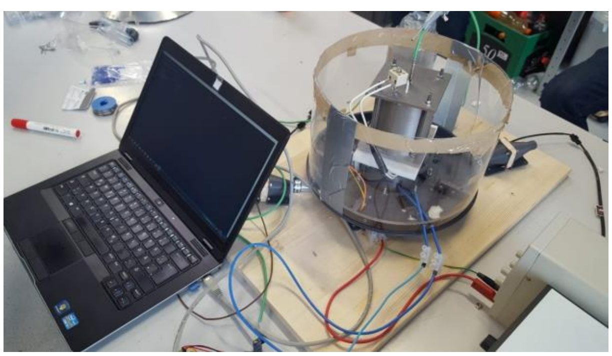

Fig. 16: First prototype of the spinning apparatus. External power supply was used for the heating system and to power the spinning motor. Spinning was done at nominal speed of 600 rpm.

Despite extremely simple prototype that were used for the first tests, specimen of E-glass fibers were spun. These fibers have a diameter of 20 µm, but they were brittle and no longer than 30 mm. The brittleness may be due to insufficiently hot nozzles and accordingly partially crystalized fibers. Additionally, E-glass reacted with the stainless-steel and the fiber structure contain impurities. Both effects should be removed by using the PtRh bushing, which has higher thermal conductivity than stainless steel and doesn't react with glass at high temperatures. Tests using the 3D-printed PtRh bushing have still not been conducted. Fig. 17 shows a fiber as it hangs from the bushing assembly after the rotation of the spinning apparatus was stopped. Fig. 18 shows the fibers spun during this test. Therefore, the centrifugal spinning concept was verified and the design frozen.

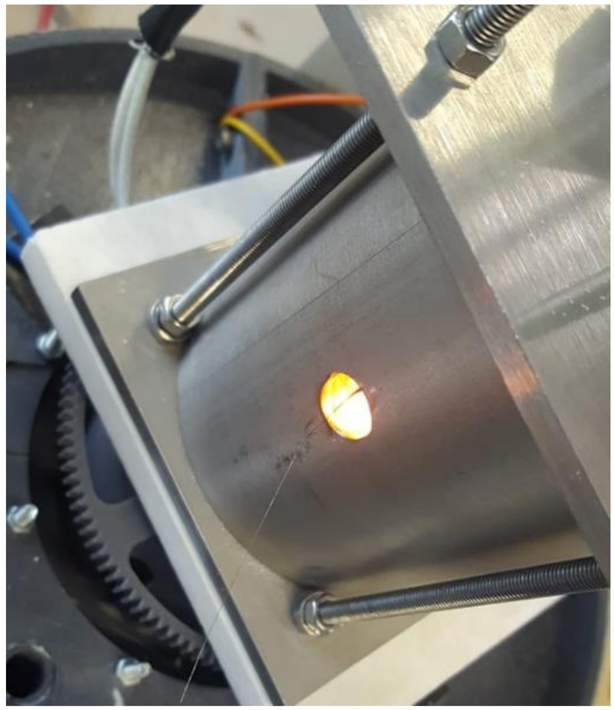

Fig. 17: E-glass fiber hanging for the bushing after the spinning test. Note the 3D-printed drive gear of the spinning apparatus and the white Teflon plate used to insulate it from the stainless-steel enclosure of the bushing assembly.

Fig. 18: Multiple E-glass fibers spun during the first spinning tests.

3.3. Cooling system tests

The cooling system was tested next. The same spinning apparatus as shown in Fig. 16 was placed in a plexiglass enclosure. Same heating procedure was conducted as for the previous spinning tests, only that this time three coolers were used to circulate the air from outside through the enclosure in order to heat the system. The goal was to determine the time until the plexiglass top reaches its melting temperature of 160 °C. After 20 minutes, how long the spinning tests lasted, this did not occur, so the team proceeded to further heat the experiment. Melting of the plexiglass top occurred after 26 minutes. While this test is not representative of the flight conditions, it showed that the cooling system is a valid concept and that the temperatures inside the pressure vessel will not reach temperatures higher than 160 °C during the 20 minutes of the experiment time. Fig. 19 shows the first test of the cooling system.

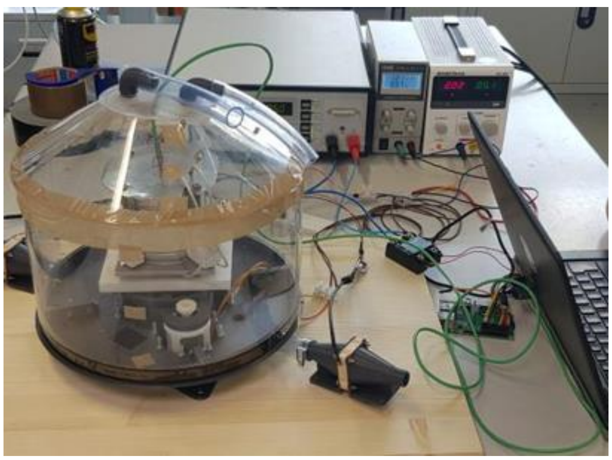

Fig. 19: First test of the cooling system. Note that fiber spinning was not attempted during this test.

Since the heat sink was not available at that point an aluminum top was added to the prototype to simulate the heat sink and thereby better approximate flight conditions. Fiber spinning was attempted in another test, using the counter-rotating catching drum as foreseen in the preliminary design [7]. It was achieved to spin fibers and it was shown that the fibers do not get attached to the drum, thus making it redundant. The cooling system this time performed as expected. The aluminum cover never reached temperatures higher than 40 °C. This prototype is shown in Fig. 20.

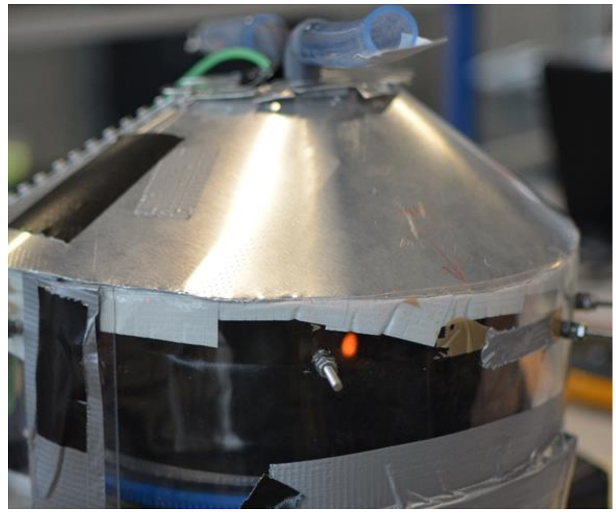

Fig. 20: The second prototype of the spinning apparatus with the cooling system during the heating procedure. Note the glowing bushing assembly and the aluminum top of the prototype.

Further testing using these simple prototypes was concluded unnecessary since the crucial functional aspects were proven. The only aspect that could not have been tested was the heat distribution inside the heat sink through the paraffin PCM, since the 3D-printed heat sink was unavailable. To determine the optimal lattice structure for the design of the heat sink, EOS GmbH provided 5 different aluminum lattice specimens. These were filled with n-Octadecane paraffin wax [14] and heated from on the one side. One side of the specimen was fitted with a Germanium window so that the heat distribution through the lattice could be observed using an IR camera. Fig. 21 shows the 4 out of 5 specimens. Fig. 22 shows the test assembly and the IR camera. Fig. 23 shows the heat distribution through the lattice structure.

Fig. 21: 4 lattice specimens, each 50 x 50 x 50 mm in size. One open side is left to be covered by germanium window.

Fig. 22: Initial test setup with the IR camera and one thermally insulated lattice specimen filled with paraffin.

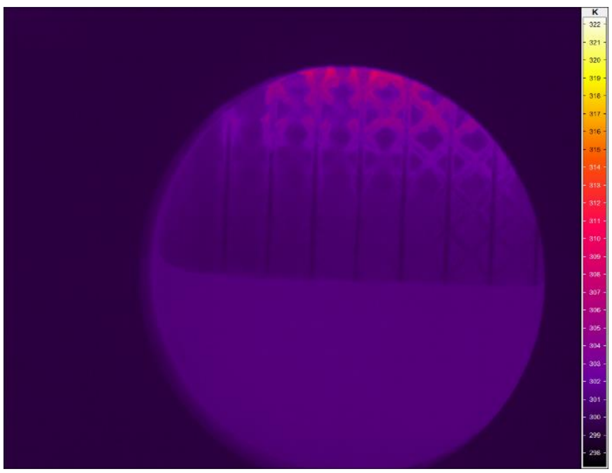

Fig. 23: Heat distribution through the lattice as seen by the IR camera during the initial tests. Note that the heating element is placed on the upper side of the lattice specimen. The molten paraffin can be seen obscuring the lower side of the lattice.

These initial tests show that the aluminum lattice distributes the heat through the whole mass of the paraffin. For the final design of the heat sink, the f2ccz lattice was chosen. The heat sink can be considered as experiment on its own. The exact design, test procedure and conclusions from those tests will be provided in another future publication.

3.4. Tests of an alternative heating system

The heating wire concept cannot be verified before being tested on a shaker test bench. Another alternative heating system concept has been designed in case the heating wire fails due to the vibration loads. Instead of a Kanthal A1 heating wire wound around the bushing, two heating elements used on the EXOMars rover are proposed. These elements use a platinum heating wire embedded in a ceramic cylindrical casing with an inner diameter of 6 mm. One such element was tested on a nozzle of the stainless-steel bushing. Both parts were embedded in UltraBoard® as shown in Fig. 24. The goal of the heating tests was to achieve the required temperature of 1250°C inside the PtRh bushing within 20 minutes.

Fig. 24: 3D-printed stainless-steel bushing printed by EOS GmbH with the heating element. Note that the flight model of the bushing has two nozzles instead on one.

This heating test was performed at 87.6 W at 2.3 A. After 330 s a temperature of 1272 °C was reached. Recall that the heating system using the heating wire reached temperatures of 1180 °C after 20 minutes at 200 W. The better performance of the heating element is partly due to better insulation and a smaller bushing mass. The heating element failed after 330 s. Upon inspection, it was discovered that the bushing material melted, which is likely the cause of the failure. Furthermore, the heating element was used beyond its maximum operation conditions. Fig. 25 shows the test assembly after the heating. Fig. 26 shows the heated bushing compared to a new one. Fig. 27 shows the heating element after the heating.

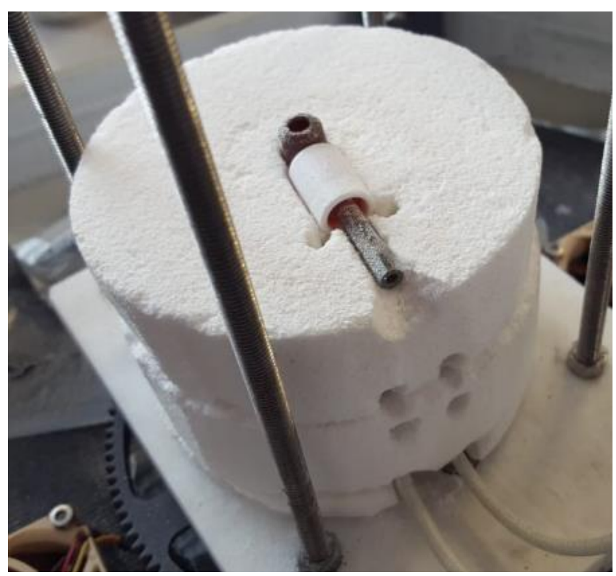

Fig. 25: The test assembly shortly after the failure of the heating element. Note that the bushing is still glowing.

Fig. 26: Failed heated bushing (left) compared to a new one (right)

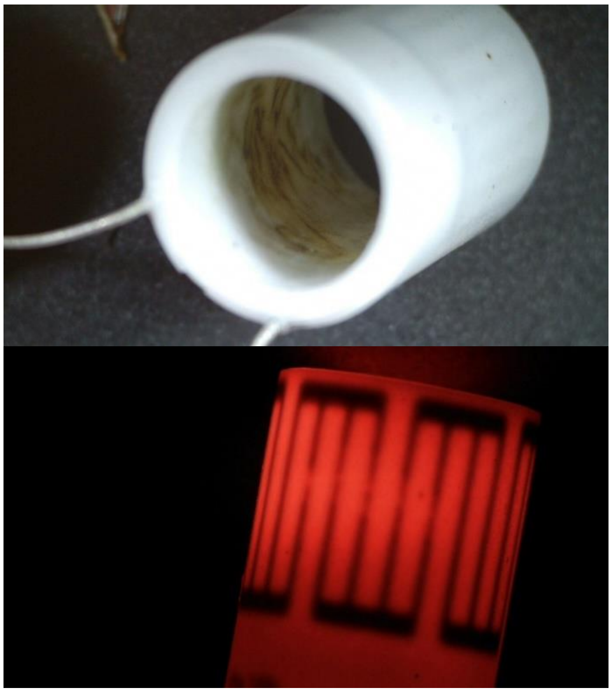

Fig. 27: Failed heating element (top) and the burned through sections of the heating wire embedded into the element (bottom).

The desired temperature of 1250 °C could be achieved within 20 minutes with the heating elements, thus providing an alternative to the heating wire concept. At the same time, this heating element is substantially more resistant to vibrations.

4. Conclusion and outlook

In this work the final design of the IMFEX experiment is presented. Changes were made compared to the preliminary design published by *Krämer et al* [7]. Tests that have been performed to verify design decisions and increase the maturity of the concepts are described.

Upon manufacturing all the components of the final design, further tests will be performed on the sub-system and system level. Most relevant tests that need to be performed are those on the 3D-printed heat sink, since these tests could not have been done before. Both heating systems have to be tested on the new PtRh bushing and on the shaker-test bench. After these tests are completed, the final decision will be made which of these two systems should be used for the flight model. Next steps are flight qualification of the whole experiments on a shaker test bench and inside a thermal vacuum chamber.

Acknowledgements

Project IMFEX is part of German/Swedish REXUS/BEXUS program. The team is supported by the team of the *MoonFibre* project, namely by the Institute for Structural Mechanics and Lightweight Design of RWTH Aachen University (SLA) and Institut für Textiltechnik of RWTH Aachen University (ITA). Both institutes provide assistance with the experiment concept development, manufacturing and testing. Furthermore, the team is supported by EOS GmbH and Cooksongold, both of which provided the team with additive manufacturing capability. EOS GmbH printed the Aluminum heat sink and Cooksongold the PtRh bushing. The team is also supported by Lava-X, who will weld all the experiment's aluminum parts, including the ones printer by EOS. Lastly, IMFEX was provided with high-temperature insulation materials from Schupp Ceramics.

References

[1] B. Dunbar, *What is Artemis?* [Online]. Available: https://www.nasa.gov/what-is-artemis (accessed: Dec. 17 2019).

[2] S. Potter, *NASA Names Companies to Develop Human Landers for Artemis Missions.* [Online]. Available: https://www.nasa.gov/press-release/nasa-names-companies-to-develop-human-landers-for-artemis-moon-missions (accessed: Sep. 29 2020).

[3] H. Benaroya, *Building habitats on the Moon: Engineering approaches to lunar settlements / Haym Benaroya*. Cham, Switzerland: Springer, 2018.

[4] E. Mahoney, *In-Situ Resource Utilization.* [Online]. Available: https://www.nasa.gov/isru (accessed: Dec. 19 2019).

[5] S. Panajotovic, T. Meinert, T. A. T. Becker, J. C. A. Romero, and A. Lüking, "MoonFibre - Fibres from Lunar Regolith," in *18th Space Generation Congress, Washington DC, 2019.* [Online]. Available: https://publications.rwth-aachen.de/record/775244

[6] Alvaro Blay Sempere, "Production of synthetic Moon soils and their fiberization for lunar settlement applications," Bachelor Thesis, Institut für Textiltechnik, RWTH Aachen University, Aachen, 2016.

[7] C. Krämer *et al.*, "Design of a Moonfibre Spinning Apparatus for the Use on a REXUS Research Rocket," in *Aerospace Europe Conference*, Bordeaux, France, 2020.

[8] *Fiber Optics | Made In Space.* [Online]. Available: https://madeinspace.us/capabilities-and-technology/fiber-optics/ (accessed: Jan. 10 2020).

[9] REXUS/BEXUS Student Experiment Programme, *REXUS: Rocket EXperiments for University Students.* [Online]. Available: http://rexusbexus.net /rexus/ (accessed: Jan. 11 2020).

[10] M. M. Farid, A. M. Khudhair, S. A. K. Razack, and S. Al-Hallaj, "A review on phase change energy storage: materials and applications," *Energy Conversion and Management*, vol. 45, 9-10, pp. 1597–1615, 2004, doi: 10.1016/j.enconman.2003.09.015.

[11] A. Abhat, "Low temperature latent heat thermal energy storage: Heat storage materials," *Solar Energy*, vol. 30, no. 4, pp. 313–332, 1983, doi: 10.1016/0038-092X(83)90186-X.

[12] Daxi Xiong, "An experimental study of the cooling of a thin glass fibre during formation process," *Experimental Heat Transfer*, pp. 31-46, 2010, doi: 10.1080/08916150490246537

[13] Sergey I. Gutnikov and Bogdan I. Lazoryak, "Effect of Nozzle Diameter on Basalt Continuous Fiber Properties," in *Advances in Glass Fibers*, vol. 65, no. 7, 2019, doi: 10.3390/fib7070065

[14] *n-Octadecane 820920.* [Online]. Available: https://www.sigmaaldrich.com/catalog/product/mm/820920?lang=de&region=DE (accessed: Jan. 13 2020).